Available online at www.sciencedirect.com
ScienceDirect
Ceramics International 35 (2009) 143–146
CERAMICS INTERNATIONAL
www.elsevier.com/locate/ceramint

Structure, dielectric and optical properties of $Bi_{1.5+x}ZnNb_{1.5}O_{7+1.5x}$ pyrochlores

Qian Wang, Hong Wang *, Xi Yao

Electronic Materials Research Laboratory, Key Laboratory of the Ministry of Education, Xi'an Jiaotong University, Xi'an 710049, China

Accepted 1 October 2007
Available online 23 December 2007

Abstract

Non-stoichiometric pyrochlore ceramics with formula $Bi_{1.5+x}ZnNb_{1.5}O_{7+1.5x}$ were systematically investigated. Crystal structures of the compounds were studied by X-ray diffraction (XRD) technique. The structures were identified as pure cubic pyrochlores when $|x| < 0.1$. Dielectric and optical properties of the compositions when $x = -0.1$, 0 and 0.1 were studied. All samples have high resistivities and low dielectric loss. With increasing x in $Bi_{1.5+x}ZnNb_{1.5}O_{7+1.5x}$, the lattice constant, permittivity, temperature coefficient of permittivity and thermal expansion coefficient increased, while dielectric loss decreased. Raman spectra indicated that the intensity of Bi–O stretching become stronger with increasing x. A vibration mode emerging at 861 cm^{-1} when $x = -0.1$ means that the B–O coordination environment is significantly more disordered. Absorption spectra suggested that the bandgap energy become lower from 2.86 to 2.70 eV as lattice constants increased. Strong absorption occurs at wavelengths from 433 to 459 nm, shows that samples have the ability to respond to wavelengths in the visible light region.

Keywords: C. Dielectric properties; C. Optical properties; BZN pyrochlores; Non-stoichiometric

1. Introduction

A large number of pyrochlore analogs have been synthesized with an amazing variety of chemical compositions and exploitable properties. These include dielectric, ferroelectric, piezoelectric, ferromagnetic, anti-ferromagnetic materials, temperature-stable high-permittivity properties, catalytic behavior, colossal magneto-resistance (CMR), etc. [1]. In 1931, Von Gaertner et al. described the structure of the ideal oxide pyrochlores. The overall formula of pyrochlore is $A_2B_2O_7$, and it is often written as $A_2B_2O_6O'$ to distinguish the oxygen atoms in the two different networks A_2O' and B_2O_6. The A_2O' network features four-coordinate O′ ions and two-coordinate A cations. The B_2O_6 framework consists of [BO_6] octahedral sharing all vertices to form large cavities [2,17]. In 1970s, bismuth-based pyrochlore compounds of Bi_2O_3–ZnO–Nb_2O_5 (BZN) ternary system for multilayer capacitors were explored in Chinese industry. And then in 1990s, two pyrochlore phases in BZN system were found in our laboratory. One of these is crystallized as cubic pyrochlore with formula $Bi_{1.5}ZnNb_{1.5}O_7$. The system attracted much attention for the excellent properties such as low sintering temperature (below 1000 °C), high dielectric constant (∼150), low loss (∼10^{-4}) and tunable temperature coefficient. It is of considerable importance for numerous applications including capacitive components, LTCC, multiplied filters, phase shifters and microwave (MW) passive components [3–6,16].

This paper focuses on non-stoichiometric BZN pyrochlores with formula $Bi_{1.5+x}ZnNb_{1.5}O_{7+1.5x}$, where $x = -0.1$, 0 and 0.1. The relationship between the compositions and properties was investigated. The Raman spectra and the absorption spectra were measured to obtain more information.

2. Experimental procedure

$Bi_{1.5+x}ZnNb_{1.5}O_{7+1.5x}$ samples were prepared by conventional solid-state powder processing techniques, which includes mixing, calcining, pulverizing, palletizing and sintering steps. The samples were sintered at 1000 °C for 3 h. Phase structures of the sintered ceramics were studied by X-ray diffractometer (Rigaku, Dmax-2400), Cu Kα, 40 kV–10 mA, 10–80°. The

* Corresponding author at: Xi'an Jiaotong University, Key Laboratory of the Ministry of Education, Electronic Materials Research Laboratory, Xi'an 710049, China.
E-mail address: hwang@mail.xjtu.edu.cn (H. Wang).

0272-8842/$34.00
doi:10.1016/j.ceramint.2007.10.028

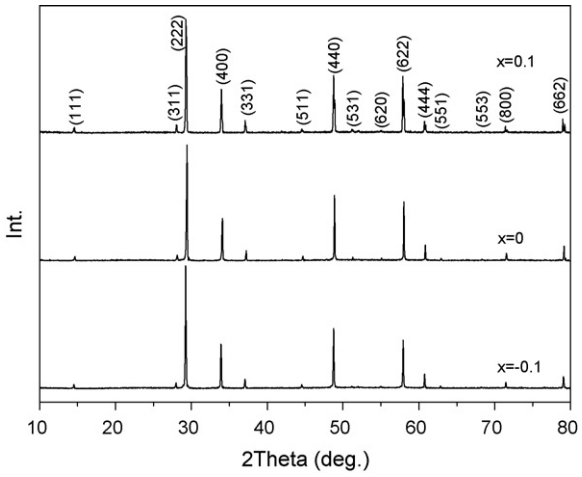

Fig. 1. X-ray diffraction patterns of the $Bi_{1.5+x}ZnNb_{1.5}O_{7+1.5x}$ ceramic discs sintered at 1000 °C.

powder diffraction lines of mixture (Silicon and BZNT) in the 2θ range of 60–120° were collected and used for lattice refinement using silicon as an internal standard. The capacitance versus frequency and temperature characteristics were measured using HP 4284A impedance analyzer. Resistance data were obtained using HP 4339A high-resistance meter under dc voltage of 100 V. Thermal expansion coefficients were measured by NETZSCH DIL 402C diffractometer. Raman spectra were recorded by a Jorbin Yvon HR800 FT-Raman spectrometer in the Raman shift range of 100–1000 cm^{-1} with a spectral resolution of 2 cm^{-1}. Reflect spectra were measured by a JASCO V-570 UV/VIS/NIR spectrophotometer with ISN-470 integrating sphere accessory at room temperature.

3. Results and discussion

3.1. Phase structure

The structures of the non-stoichiometric $Bi_{1.5+x}ZnNb_{1.5}O_{7+1.5x}$ pyrochlores were evaluated to be single phase structures when $|x| < 0.1$. The X-ray diffraction (XRD) patterns are shown in Fig. 1. All the peaks could be indexed as cubic pyrochlore with space group *Fd3m*. The lattice constant was determined using the relation:

$$a = \frac{d}{\sqrt{h^2 + k^2 + l^2}} \quad (1)$$

where d is the interplanar distance in Å and h, k, l are planes. The value of lattice constant is calculated from 90° to 120° degree 2θ angle peaks. The corrected value of lattice parameter was extrapolated versus $\cos^2\theta(1/\theta + 1/\sin\theta)$, as shown in Table 1. Increasing Bi^{3+} concentration in $Bi_{1.5+x}ZnNb_{1.5}O_{7+1.5x}$ compounds results in the increase of lattice constants. It is due to the large radius of Bi^{3+}.

3.2. Dielectric and thermal properties

The dielectric and thermal properties of the compositions are shown in Table 1. All the samples exhibit low dielectric loss and high resistivity. The low dielectric loss is attributed to the single pyrochlore phase structure [7]. The dielectric constants are about 150 and the temperature coefficients are negative around −500 ppm/°C. There is a strong correlation when Nb^{5+} is placed in the center of octahedra and would result in high ε and large negative α_ε [8]. There is direct relationship between dielectric properties and Bi^{3+} concentration. The dielectric constants and negative temperature coefficients of dielectric constants increased with increasing x.

Thermal expansion coefficients decreased with increasing x. Ruffa [9] pointed out that thermal expansion coefficient is in direct proportion to the distance of two adjacent atoms. It is a parameter closed to the metal-oxide ionic bond length, which is in direct ratio to the lattice constant.

3.3. Raman spectra

The crystalline samples were also examined by Raman spectroscopy to search for short-range structural differences. The Raman spectra of the four samples are shown in Fig. 2. The shapes of Raman spectra of the samples are similar as they mainly correspond to the pyrochlore structures [10]. The bands are assigned to symmetry species in Table 2 compared to the previously published literatures [11,12]. The bands at 182 and 248 cm^{-1} are assigned to the A–O stretching. The bands at 760 and 977 cm^{-1} are associated with the B–O stretching vibration in the BO_6 octahedron. Begg et al. [13] regards that a new shift at 861 cm^{-1} is the vibration mode originating from the localized short-range disorder of B site atoms. This new vibration mode emerging at $x = -0.1$ means that the B–O coordination environment is significantly more disordered.

With an increase in x value, the Bi^{3+} concentration increases and the intensity of Bi–O stretching become stronger. It is known that the intensity of Raman diffusion is in direct proportion to the polarizability, and the polarizability increases following the lattice constant, which results in the increasing of Bi–O stretching intensity.

Table 1
Lattice constants and dielectric parameters in series ceramics

Sample (x)	a (Å)	ε at 1 MHz	tgδ at 1 MHz ($\times 10^{-4}$)	α_ε at 125 °C 1 MHz (ppm/°C)	ρ ($\times 10^{15}$ ΩΥcm)	TEC at 400 °C ($\times 10^{-6}$ (°C)$^{-1}$)	E_g (eV)
−0.1	10.5481	142	4.2	−483	5.7	4.85	2.86
0	10.5530	148	6.5	−513	1.0	5.35	2.83
0.1	10.5609	164	2.7	−560	1.8	5.41	2.70

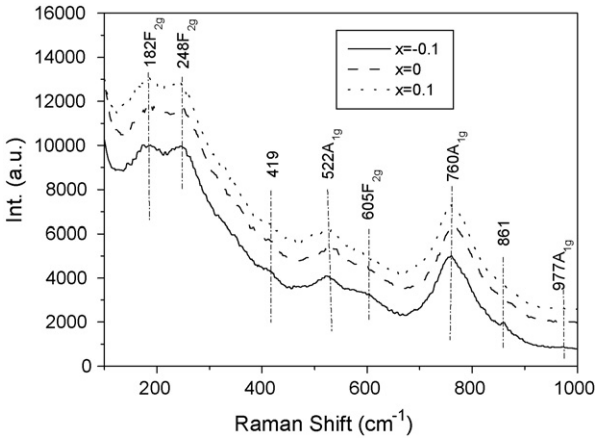

Fig. 2. Raman spectra of samples at room temperature.

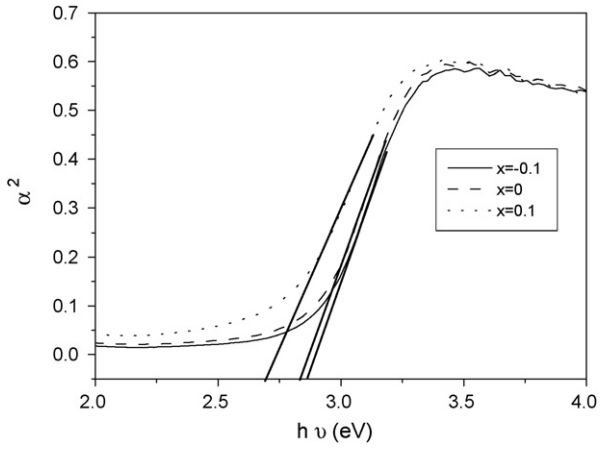

Fig. 3. Absorption spectra calculated from the reflectance data of samples.

3.4. Absorption spectra

Reflectance spectra were measured to evaluate bandgap energy refers to the valence-band to conduction-band edge transition. Fig. 3 shows the absorption spectra calculated from the reflectance data. The exponential absorption edge called Urbach edge is derived from optical phonons and lattice vibration in most ionic solids [14]. The Urbach edge moving to the lower photon energy is caused by the extension of lattice constant [15]. The bandgap energy can be estimated from the following equation by assuming a direct transition between the bands [18]:

$$\alpha = \frac{A(h\upsilon - E_g)^{1/2}}{h\upsilon} \quad (2)$$

where α is the absorbance coefficient, $h\upsilon$ is photon energy and A is a constant. The bandgap energy E_g was determined by extrapolating the straight regions of the absorption band to $h\upsilon$ axis at zero absorption value shown in Table 1, suggesting that the bandgap energy shows appreciate redshift when increasing x. The absorption wavelength can be calculated by the following formula:

$$\lambda_0\,(\mathrm{nm}) = \frac{1240}{E_g\,(\mathrm{eV})} \quad (3)$$

The compounds show optical absorption at wavelength between 433 and 459 nm. This means that the compounds have the ability to respond to wavelengths in the visible light region.

Table 2
Observed Raman shift (cm^{-1}) and assignment for the samples

Bands	Species	Assignment
182	F_{2g}	Bi–O stretching
248	F_{2g}	Zn–O stretching
419	A_{1g}	Not defined
522	A_{1g}	O–B–O bond bend
760	A_{1g}	Nb–O stretching
977	A_{1g}	Zn–O stretching

4. Conclusions

Crystal structure, dielectric and optical properties of $Bi_{1.5-x}ZnNb_{1.5}O_{7-1.5x}$ were studied. The XRD patterns can be indexed as the single cubic pyrochlore structures when $|x| < 0.1$. The lattice constants increase gradually with increasing x due to the big radius of Bi^{3+}. The low dielectric loss is attributed to the single pyrochlore phase structure. The dielectric constants and negative temperature coefficients of dielectric constants increased with increasing bismuth content. Thermal expansion coefficients decreased as in direct relationship with lattice constant. The intensity of Bi–O stretching in Raman spectra becomes stronger when increasing the concentration of bismuth. A new vibration mode emerging at 861 cm^{-1} when $x = -0.1$ means that the B–O coordination environment is significantly more disordered. The exponential absorption edges show appreciate redshift with the extension of lattice constant suggesting that the bandgap energy become lower with x increasing. Values of absorption wavelength are from 433 to 459 nm, suggested that the samples have the ability to respond to wavelengths in the visible light region.

Acknowledgement

This work was supported by National 973-project of China under grant 2002CB613302 and NSFC project of China under grant 50572085.

References

[1] T.A. Vanderah, I. Levin, An unexpected crystal-chemical principle for the pyrochlore structure, Eur. J. Inorg. Chem. (2005) 2895–2901.
[2] H. Von Gaertner, Neues jahrb, mineral geol, Palaeontol 61 (1931) 1–15.
[3] C.A. Randall, J.C. Nino, M.T. Lanagan, et al., Bi-pyrochlore and zirconolite dielectrics for integrated passive component applications, Am. Ceram. Soc. Bull. (November) (2003) 9101–9108.
[4] W. Ren, S. Trolier-Mckinstry, C.A. Randall, T.R. Shrout, Bismuth zinc niobate pyrochlore dielectric thin films for capacitive applications, J. Appl. Phys. 89 (1) (2001) 767–774.
[5] J.-H. Park, S.-H. Son, et al., Bismuth–zinc–niobate embedded capacitors grown at room temperature for printed circuit board applications, Appl. Phys. Lett. 88 (2006) 192902.

[6] J.H. Park, W.S. Lee, N.J. Seong, et al., Distributed phase shifter with pyrochlore bismuth zinc niobate thin films, IEEE Microw. Wireless Compon. Lett. 16 (5) (2006) 264–266.
[7] R. Christoffersen, P.K. Davies, Effect of Sn substitution on cation ordering in $(Zr_{1-x}Sn_x)TiO_4$ microwave dielectric ceramics, J. Am. Ceram. Soc. 77 (6) (1994) 1441–1450.
[8] B. Melot, E. Rodriguez, et al., Displacive disorder in three high-k bismuth oxide pyrochlores, Mater. Res. Bull. 41 (2006) 961–966.
[9] A.R. Ruffa, Thermal expansion in insulating materials, J. Mater. Sci. 15 (1980) 2258–2267.
[10] H. Du, X. Yao, Structural trends and dielectric properties of bi-based pyrochlores, J. Mater. Sci. Mater. Electron. 15 (2004) 613–616.
[11] H. Wang, H. Du, X. Yao, Structural study of Bi_2O_3–ZnO–Nb_2O_5 based pyrochlores, Mater. Sci. Eng. B 99 (2003) 20–24.
[12] S.M. Zanetti, S.A. da Silva, G.P. Thim, A chemical route for the synthesis of cubic bismuth zinc niobate pyrochlore nanopowders, J. Solid State Chem. 177 (2004) 4546–4551.
[13] B.D. Begg, N.J. Hess, W.J. Weber, Heavy-ion irradiation effects in $Ca_2(Ti_{2-x}Zr_x)O_7$ pyrochlores, J. Nuclear Mater. 289 (2001) 188–193.
[14] J.D. Dow, D. Redfield, Toward a unified theory of Urbach's rule and exponential absorption edges, Phys. Rev. B 5 (2) (1972) 594–610.
[15] B. Welber, M. Cardona, Dependence of the direct energy gap of GaAs on hydrostatic pressure, Phys. Rev. B 12 (12) (1975) 5729–5738.
[16] H. Wang, S. Kamba, H. Du, M. Zhang, X. Yao, Microwave dielectric relaxation in cubic bismuth based pyrochlores containing titanium, J. Appl. Phys. 100 (2006) 014105.
[17] X. Wang, H. Wang, X. Yao, Structures, phase transformations, and dielectric properties of pyrochlores containing bismuth, J. Am. Ceram. Soc. 80 (10) (1997) 2745–2748.
[18] D.H. Bao, X. Yao, Band-gap energies of sol–gel-derived $SrTiO_3$ thin films, Appl. Phys. Lett. 79 (23) (2001) 3767–3769.